The Plant Cell, Vol. 20: 3374–3388, December 2008, www.plantcell.org

Arabidopsis Synaptotagmin 1 Is Required for the Maintenance of Plasma Membrane Integrity and Cell Viability [W]

Arnaldo L. Schapire,[a,1] Boris Voigt,[b,c,1] Jan Jasik,[c] Abel Rosado,[a,2] Rosa Lopez-Cobollo,[d] Diedrik Menzel,[c] Julio Salinas,[d,e] Stefano Mancuso,[b] Victoriano Valpuesta,[a] Frantisek Baluska,[c] and Miguel A. Botella[a,3]

[a] Departamento de Biología Molecular y Bioquímica, Universidad de Málaga, 29071 Málaga, Spain
[b] Department of Horticulture, University of Florence, 50019 Sesto Fiorentino, Italy
[c] Institute of Cellular and Molecular Botany, University of Bonn, 53115 Bonn, Germany
[d] Departamento de Biotecnología, Instituto Nacional de Investigacion y Tecnologia Agraria y Alimentaria, 28040 Madrid, Spain
[e] Departamento de Biología de Plantas, Centro de Investigaciones Biológicas–Consejo Superior de Investigaciones Cientificas, 28040 Madrid, Spain

Plasma membrane repair in animal cells uses synaptotagmin 7, a Ca^{2+}-activated membrane fusion protein that mediates delivery of intracellular membranes to wound sites by a mechanism resembling neuronal Ca^{2+}-regulated exocytosis. Here, we show that loss of function of the homologous *Arabidopsis thaliana* Synaptotagmin 1 protein (SYT1) reduces the viability of cells as a consequence of a decrease in the integrity of the plasma membrane. This reduced integrity is enhanced in the *syt1-2* null mutant in conditions of osmotic stress likely caused by a defective plasma membrane repair. Consistent with a role in plasma membrane repair, SYT1 is ubiquitously expressed, is located at the plasma membrane, and shares all domains characteristic of animal synaptotagmins (i.e., an N terminus-transmembrane domain and a cytoplasmic region containing two C2 domains with phospholipid binding activities). Our analyses support that membrane trafficking mediated by SYT1 is important for plasma membrane integrity and plant fitness.

INTRODUCTION

The plasma membrane is a biological barrier between the extracellular and intracellular environments and is essential for the maintenance of cell integrity. If the plasma membrane is not properly resealed following damage, cell death is the rapid and invariant outcome (Bement et al., 2007). In fact, plasma membrane disruption and resealing are normal events in the life of many animal cells engaged in physical activity, such as mammalian skeletal and cardiac muscle cells (Steinhardt et al., 1994; Reddy et al., 2001; McNeil and Kirchhausen, 2005). Therefore, resealing is a necessary rapid response that allows cells to survive membrane disruption, preventing the loss of irreplaceable cell types (Steinhardt et al., 1994; McNeil and Kirchhausen, 2005; Bement et al., 2007). Small disruptions, on the nanometer scale, are thought to be resealed passively as a result of thermodynamically driven lipid interactions. However, for large disruptions, in the micrometer diameter range, resealing requires exocytotic addition of internal membrane to the cell surface (Bi et al., 1995; Miyake and McNeil, 1995).

In nature, plants are subjected to changing environmental conditions during their life cycle. As a result, plants have evolved intricate mechanisms to perceive external signals, allowing optimal responses (Hasegawa et al., 2000; Zhu, 2002; Borsani et al., 2003; Baena-González et al., 2007). A successful approach to identify essential genes and processes required for abiotic stress tolerance has been the use of mutant analysis (Liu and Zhu, 1998; Shi et al., 2000; Xiong and Zhu, 2001; Borsani et al., 2002; Rubio et al., 2004; Rosado et al., 2006a). This approach allowed the identification of genes required for salt tolerance, such as the *SOS* genes; osmotic tolerance, such as the *OSM1*/*SYP61* gene; cold tolerance, such as *ICE1*; and oxidative stress tolerance, such as *ENH1* (Liu and Zhu, 1998; Liu et al., 2000; Shi et al., 2000; Chinnusamy et al., 2003; Rubio et al., 2004; Koiwa et al., 2006; Rosado et al., 2006b; Zhu et al., 2007). Although nonoptimal or stressful growing conditions could result in the damage of plasma membrane, genes putatively involved in plasma membrane repair have not been identified as abiotic stress determinants in the genetic screenings described above.

Synaptotagmins constitute a family of membrane-trafficking proteins that are characterized by an N-terminal transmembrane region, a linker of variable size, and two C-terminal C2 domains in tandem (Craxton, 2004). C2 domains, identified as a conserved sequence motif in protein kinase C (Coussens et al., 1986), are autonomously folded protein modules that generally act as Ca^{2+} and phospholipid binding domains and were shown to represent

[1] These authors contributed equally to this work.
[2] Current address: Department of Botany and Plant Sciences, Institute for Integrative Genome Biology, Center for Plant Cell Biology, University of California, Riverside, CA 92521.
[3] Address correspondence to mabotella@uma.es.
The author responsible for distribution of materials integral to the findings presented in this article in accordance with the policy described in the Instructions for Authors (www.plantcell.org) is: Miguel A. Botella (mabotella@uma.es).
[W] Online version contains Web-only data.
www.plantcell.org/cgi/doi/10.1105/tpc.108.063859

autonomously folded Ca^{2+} binding domains in synaptotagmins (Sutton et al., 1995). In mammals, 16 synaptotagmins have been identified, although they may show a tissue-specific isoform distribution (Südhof, 2001; Craxton, 2004; Sagi-Eisenberg, 2007). Synaptotagmin 1 (syt1), the most comprehensively characterized synaptotagmin, acts as a Ca^{2+} sensor in neurotransmitter release through its two C2 domains, and its Ca^{2+}-dependent phospholipid binding is necessary for function (Tang et al., 2006). Another well-characterized synaptotagmin in animals is syt7. Syt 7 protein is found in the membrane of lysosomes and some nonsynaptic secretory granules, where it regulates Ca^{2+}-triggered exocytosis and plasma membrane repair (Reddy et al., 2001; Andrews, 2005; Andrews and Chakrabarti, 2005). Genes encoding proteins with a similar domain architecture as well as sequence similarity to synaptotagmin C2 domains have also been found in plant genomes (Craxton, 2004, 2007), although their function remains unknown.

In this study, we report the isolation of an *Arabidopsis thaliana* mutant, *syt1*, which shows hypersensitivity at high NaCl concentrations. The identification of the mutated gene revealed that it encodes a protein with homology to animal synaptotagmins. The *Arabidopsis SYT1* gene shows ubiquitous expression, and the SYT1 protein is preferentially located at the plasma membrane. Our biochemical data reveal that the C2 domains of SYT1 display phospholipid binding activities, a fundamental feature of synaptotagmins. Loss of function of *Arabidopsis SYT1* causes a reduction in plasma membrane integrity, which leads to a decrease in cell viability. Moreover, this reduced plasma membrane integrity is observed in *syt1* in control growing conditions and is enhanced (with respect to wild-type seedlings) under high osmolarity. Based on this study, we propose that *SYT1* is an essential component of plasma membrane repair in plants.

RESULTS

Identification of an *Arabidopsis* Synaptotagmin Gene That Is Required for NaCl Tolerance

To identify genes essential for NaCl tolerance, we performed a forward genetic screen in an *Arabidopsis* T-DNA insertion mutant population for plants hypersensitive to the presence of 160 mM NaCl (Rosado et al., 2006b). As a result, we isolated a T-DNA insertion line in the *Arabidopsis* ecotype C24 (named *syt1-1*; see below) that showed hypersensitivity to NaCl. As shown in Figure 1A, wild-type and *syt1-1* seedlings showed similar growth under control conditions. However, upon exposure to 160 mM NaCl, roots of wild-type seedlings grew slowly, while *syt1-1* root growth was inhibited even more (Figure 1A). The genomic DNA flanking the left border of the T-DNA in *syt1-1* was amplified by thermal asymmetric interlaced PCR as described previously (Liu and Whittier, 1995), revealing that the insertion was located in the 5′ untranslated region, 106 bp upstream the ATG translation start site of the *At2g20990* gene (Figure 1B). The gene contains 11 exons and 10 introns and was named *SYT1* because it encodes a protein with similar structure to animal synaptotagmins (Figure 1C) (Craxton, 2004; Sudhof, 2004). A homology search of SYT1 against the human protein reference database (Mishra et al., 2006) showed syt7 as the protein with the highest homology. Syt7 is located in the membrane of lysosomes and some nonsynaptic secretory granules, where it regulates Ca^{2+}-triggered exocytosis and plasma membrane repair (Reddy et al., 2001; Andrews, 2005; Andrews and Chakrabarti, 2005).

To confirm that *SYT1* was required for NaCl tolerance, we isolated an *Arabidopsis* mutant from the SAIL collection (SAIL_775_A08, *syt1-2*) with the T-DNA located in the 10th exon of *At2g20990* (Figure 1B). This T-DNA line also showed hypersensitivity when growing at high NaCl (see Supplemental Figure 1A online). We did not detect *SYT1* transcripts by RT-PCR in the *syt1-2* mutant (Figure 1D, top), and consistent with *syt1-2* being a null allele, SYT1 protein was not detected in protein gel blots of microsomal fractions isolated from *syt1-2* homozygous lines (Figure 1D, bottom). Because segregation and DNA gel blot analysis indicated that *syt1-1* contained several T-DNA insertions (data not shown), we decided to use the Columbia (Col-0) *syt1-2* mutant allele for further studies. Comparison of the hypersensitive phenotype of *syt1-2* to that of a complementing line transformed with the genomic fragment containing the *SYT1* gene fully demonstrated that the NaCl hypersensitive phenotype was due to a lesion in the *SYT1* gene (see Supplemental Figure 1B online).

SYT1 Is Ubiquitously Expressed

To analyze *SYT1* expression, we first compiled data using the Genevestigator database (Zimmermann et al., 2004). *SYT1* shows a constitutive expression in all tissues analyzed, and its expression is little affected by any of the factors reported in the database. RT-PCR experiments using RNA extracted from roots, shoots, rosette and cauline leaves, inflorescences, and siliques also suggested a ubiquitous expression for *SYT1* (Figure 1E).

To investigate the in planta expression patterns of *SYT1*, we generated transgenic lines containing a fused β-glucuronidase (GUS) gene under control of the *SYT1 cis*-regulatory sequences located upstream the open reading frame. The GUS expression patterns of several independent lines analyzed were very similar, and Figure 1F shows the results for a representative line. In roots of 3-d-old seedlings, all cells showed expression of *SYT1* (Figure 1F, panel a). Strong expression was found in the vascular tissue of the elongation zone and cells of the root cap. In 2-week-old plants, *SYT1* was expressed in most tissues. It was strongly expressed in the vascular tissue and epidermal cells of cotelydons and leaves (Figure 1F, panel b). *SYT1* was also highly expressed in trichomes (Figure 1F, panel c) and the root system (Figure 1F, panel d). In inflorescence, GUS activity was observed in most tissues of inflorescence stems, sepals, and stamen filaments (Figure 1F, panel e). These results of GUS activity are in agreement with the *SYT1* expression determined by RT-PCR and the Genevestigator database (Zimmermann et al., 2004).

SYT1 Protein Is Mainly Located at the Plasma Membrane

To provide clues to SYT1 function, we next investigated its subcellular localization. We used different strategies, including analysis of transient *Nicotiana tabacum* and stable *Arabidopsis* lines transformed with a *35S:SYT1:GFP* (green fluorescent

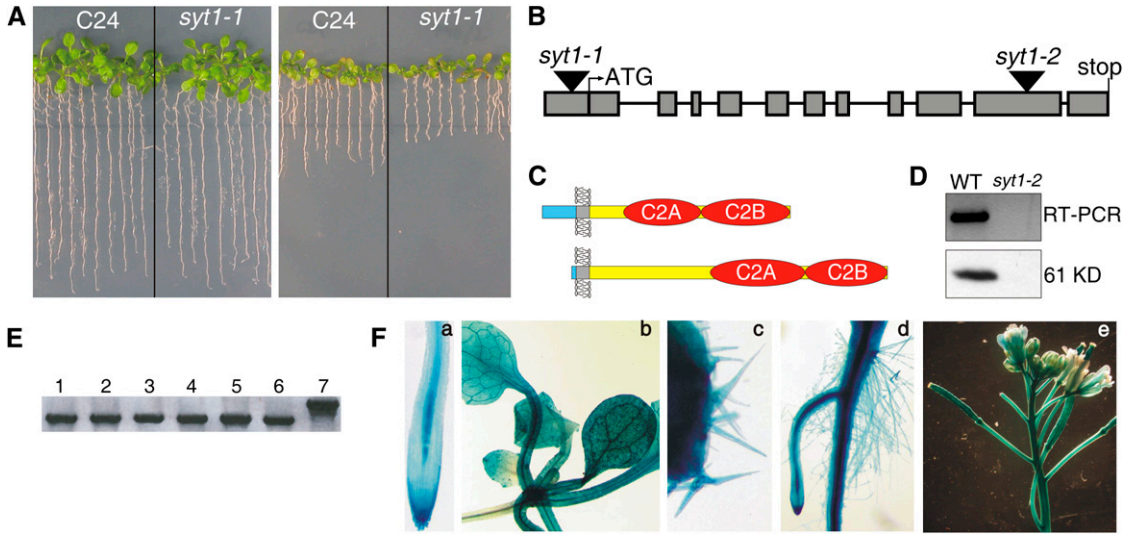

Figure 1. Identification of Mutants in the *SYT1* Gene and Expression Analyses.

(A) Wild-type C-24 and *syt1-2* seedlings were grown for 3 to 4 d in half-strength Murashige and Skoog (MS) medium (1.5 mM Ca^{2+}) and then transferred to the same medium (left panel) and medium containing 160 mM NaCl (right panel) and photographed 20 d later.
(B) T-DNA insertion sites in *syt1-2* and *syt1-2* with exons shown as gray boxes.
(C) Diagram of the structure of the animal synaptotagmins (top) and *Arabidopsis* SYT1 (bottom). SYT1 is predicted to have a short extracellular domain (blue), a transmembrane domain (gray), a linker domain (yellow), and two tandem intracellular C2 domains, C2A and C2B.
(D) RT-PCR analysis using primers flanking the T-DNA insertion in the *syt1-2* mutant (top). Immunoblots probed with antisera to SYT1 peptides indicate that no SYT1 protein is produced in *syt1-2* (bottom). The molecular weight indicated was calculated from the protein gel blot.
(E) RT-PCR analysis of *SYT1* in root (1), shoot (2), rosette leaves (3), cauline leaves (4), inflorescence (5), and silique (6). A genomic control was used (7).
(F) *SYT1* promoter-driven *GUS* expression in wild-type seedlings is observed in all tissues analyzed. **(a)** A 3-d-old seedling root; **(b)** a 2-week-old plant; **(c)** trichomes; **(d)** root of a 2-week-old plant; **(e)** inflorescence.

protein) construct as well as immunolocalization using anti-SYT1 antibodies. In leaf cells of transiently transformed tobacco, SYT1:GFP localizes to plasma membrane domains (Figure 2A) resembling elements of cortical endoplasmic reticulum. A similar pattern of expression was observed in control GFP-ER cells (see Supplemental Figure 2A online), highlighting the endoplasmic reticulum (ER) tubules like SYT1:GFP, but lacking the SYT1:GFP positive stable spots at the plasma membrane.

We also determined that the predicted transmembrane domain has an essential role in anchoring SYT1 to the plasma membrane because a transiently expressed GFP fusion protein lacking this domain is localized in the cytosol and inside the nucleus (see Supplemental Figure 2B online). Localization of SYT1:GFP to the plasma membrane is observed at distinct patches of cell periphery organizing Hechtian strands, which interconnect cell wall with the plasma membrane after plasmolysis (Figures 2B and 2C). This pattern was identical in cells of the lower epidermis of leaves and in epidermal cells at the root hair zone in stable transformed *Arabidopsis* (Figures 2D and 2E). At the root apex, there was high expression with abundant plasma membrane and cell periphery localization of SYT1 in root cap cells (Figure 2F).

Subcellular localization of SYT1 was also analyzed using the anti-SYT1–specific antibodies previously used in protein gel blot analysis (Figure 3). As a control, we used preimmune serum, indicating that the signal is specific for SYT1 (see Supplemental Figures 3A and 3B online). Localization of SYT1 in a cross section of a root apex (Figure 3A) corroborates that the SYT1 signal is associated with the plasma membrane. Especially strong SYT1-positive signals were found at the cross-walls of the transition zone of the root apex (Figure 3B), which accomplishes a high rate of endocytosis and vesicle trafficking (Baluska et al., 2005). In the shoot apex and cotyledons, there is an even distribution of SYT1 at the plasma membrane (Figures 3C and 3D). Immunogold electron microscopy confirmed localization of the SYT1 at the plasma membrane (Figures 3E and 3F). Young cell walls showed more abundant decoration of the plasma membrane with SYT1 (Figures 3E and 3F; see Supplemental Figure 2C online), and there is also abundant localization of SYT1 within plasmodesmata (Figure 3F). Our data indicate that SYT1 localizes preferentially to the plasma membrane. These results are also consistent with two previous proteomics reports that identified SYT1 in the plasma membrane using mass spectrometry (Kawamura and Uemura, 2003; Alexandersson et al., 2004).

The C2 Domains of SYT1 Show Phospholipid Binding Activity

All synaptotagmins are composed of an N-terminal transmembrane region, a central linker sequence, and two C-terminal C2 domains. The Ca^{2+}-dependent binding to phospholipid membranes is the best-characterized function of C2 domains. The

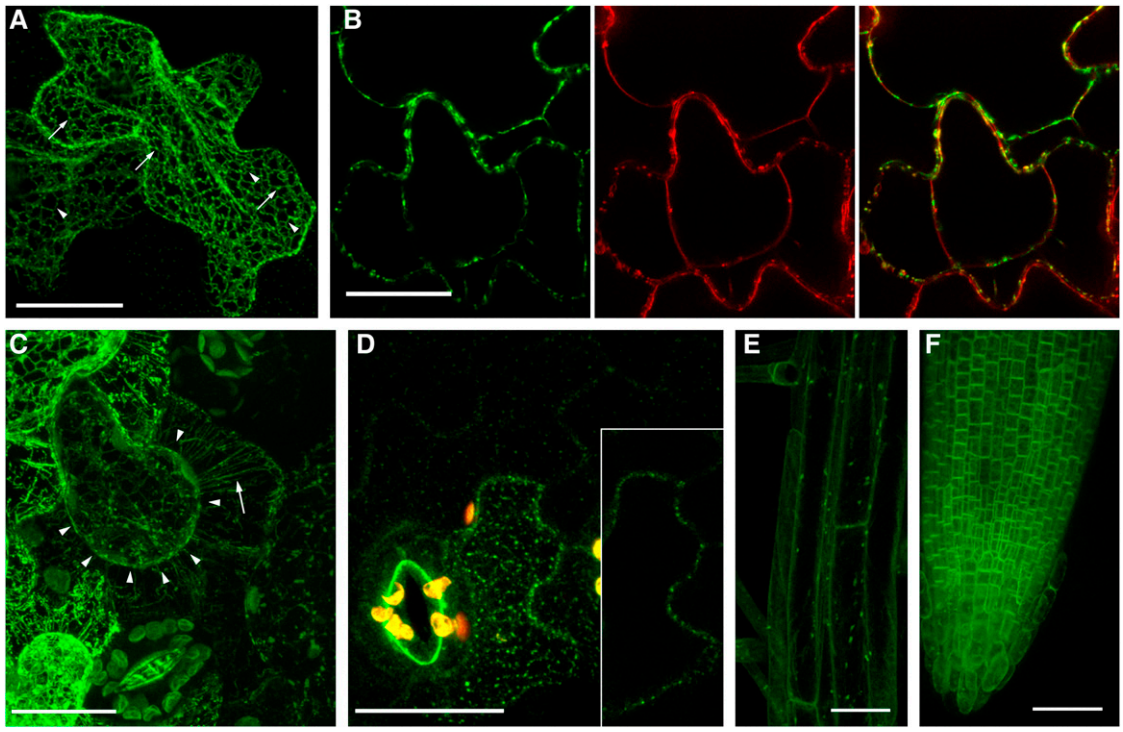

Figure 2. Subcellular Localization of SYT1.

(A) Expression of SYT1:GFP shows stable bright spots (arrows) at the plasma membrane connected by ER tubules (arrowheads). Bar = 25 μm.
(B) Leaf cells were plasmolyzed using 500 mM NaCl for 2 h. The middle of the cell is shown in a single optical section. The GFP signal remains in the retracted Hechtian strands at the plasma membrane and at the cell wall (left). FM4-64 staining of the same cell shows the stained plasma membrane and spots in the cell wall (middle). A merge of the two images reveals the colocalization of the SYT1:GFP spots to the plasma membrane and membrane positive spots at the cell wall (right). Bar = 25 μm.
(C) Projection of a salt plasmolyzed cell showing SYT1:GFP in Hechtian strands (arrow) and at the shrunken protoplast (arrowheads). Bar = 25 μm.
(D) to **(F)** Transgenic *Arabidopsis* expressing 35S-SYT1:GFP.
(D) Projection of cells of the lower epidermis of leaves. Nonmotile spots residing at the plasma membrane/cell wall are labeled. The inset shows a single optical section from the middle of the cell. Autofluorescence of open stomata cell wall and plastids appear as bright green ring and bright yellow structures, respectively. Bar = 25 μm.
(E) Detail view of epidermal cells in the elongation region. Bar = 10 μm.
(F) Projection of a root tip. Bar = 50 μm.

two C2 domains of synaptotagmins, C2A and C2B, have an independently folding, compact b-sandwich structure formed by two four-stranded β-sheets with flexible loops at the top and the bottom (Sutton et al., 1995; Fernandez et al., 2001). The conserved acidic residues (Asp) in these loops, thought to play crucial roles in coordinating Ca^{2+} ions, are also conserved in the C2A domain of SYT1 but not in the C2B domain (Figure 4A) (Shao et al., 1996; Ubach et al., 1998). Nevertheless, analyses of animal synaptotagmins indicate that Ca^{2+} and phospholipid binding properties cannot be reliably predicted from sequence analysis alone (Dai et al., 2004).

Therefore, we studied whether the C2 domains of *Arabidopsis* SYT1 are capable of forming Ca^{2+}-dependent complexes with negatively charged liposomes (25% PS/75% PC). For this purpose, we used a centrifugation assay that monitors Ca^{2+}-dependent phospholipid binding of C2 domains to liposomes (Fernández-Chacón et al., 2001). Recombinant C2 fragments of SYT1 and C2AB from rat-syt1 (used as a positive control) were purified as glutathione *S*-transferase (GST) fusion proteins and incubated with liposomes in the presence of different concentrations of free Ca^{2+}. After isolation, liposome-bound proteins were analyzed using SDS-PAGE and Coomassie blue staining. Because we could not predict the length of C2 domain required for phospholipid binding, we generated constructs with various N-terminal extensions in the C2A domain.

All SYT1-C2A peptides were capable of binding phospholipids in a Ca^{2+}-dependent manner (Figure 4B). Unexpectedly, a marked Ca^{2+}-independent binding of SYT1-C2B to liposomes was observed (Figures 4B and 4D). The binding properties of SYT1-C2AB differed from those of the single domains and behaved as a mix of the individual C2 domains (i.e., binding of liposomes in the absence of Ca^{2+}, but the binding increased approximately fourfold in the presence of Ca^{2+}) (Figures 4B and 4E). To be physiologically significant, phospholipid binding to

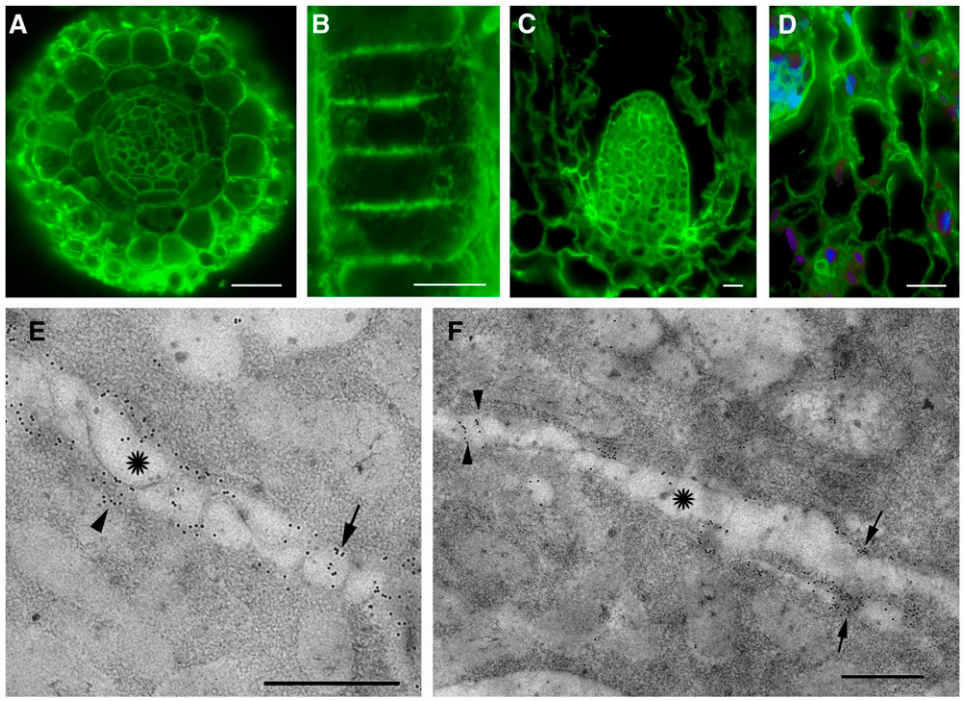

Figure 3. Preferential Plasma Membrane Localization of SYT1 Protein.

(A) to **(D)** Confocal immunohistochemical images of SYT1 in wild-type plants.
(A) Cross section of a root apex.
(B) Detailed view of cross-walls in the transition zone of the root apex enriched in SYT1:GFP. Bar = 10 μm.
(C) Shoot apex cells.
(D) Cotyledon cells. The 4',6-diamidino-2-phenylindole–positive nuclei appear as blue structures. Bars in **(A)**, **(C)**, and **(D)** = 25 μm.
(E) and **(F)** Immunogold electron microscopy localization confirms the plasma membrane localization of SYT1.
(E) Young emerging cell wall (star) with some membraneous structures as traces of the endosomal origin of cytokinetic cell plate (arrow). Note large aggregates of SYT1-positive gold particles near cell plate (arrowhead).
(F) Cell wall (star) with young plasmodesmata is decorated with the SYT1-positive gold particles (arrowheads), while more mature plasmodesmata show gold particles near their orifices (arrows). The abundance of the gold particles at the plasma membrane is lower under more mature cell wall. Bars = 500 nm.

SYT1 should be stimulated by Ca^{2+} concentrations similar to those achieved in planta. We calculated a half-maximal binding of 6 μM free Ca^{2+} for SYT1-C2A (Figure 4C), similar to the 4.1 μM Ca^{2+} we determined for rat syt1-C2AB (see Supplemental Figure 4 online), a value previously reported for rat syt1-C2AB (Fernández-Chacón et al., 2002). The half maximum binding of SYT1-C2AB was ~1 to 2 μM Ca^{2+} (Figure 4E), indicating cooperativity between the C2 domains for Ca^{2+} and phospholipid binding as also reported for neuronal syt1 (Fernandez et al., 2001; Fernández-Chacón et al., 2002).

syt1-2 Shows Reduced Growth and Increased Electrolyte Leakage Compared with the Wild Type

We identified *syt1-2* by its hypersensitivity to high NaCl (Figure 1A). We then performed a detailed physiological analysis of *syt1-2* responses to NaCl. Because SYT1 shows homology to animal Ca^{2+} sensors and presents Ca^{2+}-dependent phospholipid binding activity, NaCl responses were determined in the presence of low Ca^{2+} (0.3 mM) and high Ca^{2+} (3 mM) in the medium. *syt1-2* seedlings already showed a reduced growth compared with the wild type in control conditions (Figure 5A). However, growth inhibition of *syt1-2* was enhanced upon NaCl treatment relative to the wild type (Figure 5A). The presence of low Ca^{2+} increased the sensitivity of wild-type and *syt1-2* seedlings to NaCl. At low Ca^{2+} and 150 mM NaCl, the main root of wild-type seedlings resumed its growth while *syt1-2* root growth was arrested (Figure 5A). However, at high Ca^{2+}, growth arrest of *syt1-2* roots occurred at 200 mM NaCl (Figure 5A). This was quantified by fresh weight measurements of seedlings after NaCl treatments (Figure 5B). With the exception of 200 mM NaCl, significant differences in fresh weight between wild-type and *syt1-2* seedlings were found at all concentrations analyzed, with the highest differences occurring at 150 mM NaCl.

In animals, syt7 plays an essential role in plasma membrane repair (Reddy et al., 2001; McNeil and Kirchhausen, 2005). Therefore, we speculated that loss-of-function of *SYT1* would have a defective plasma membrane repair mechanism, resulting

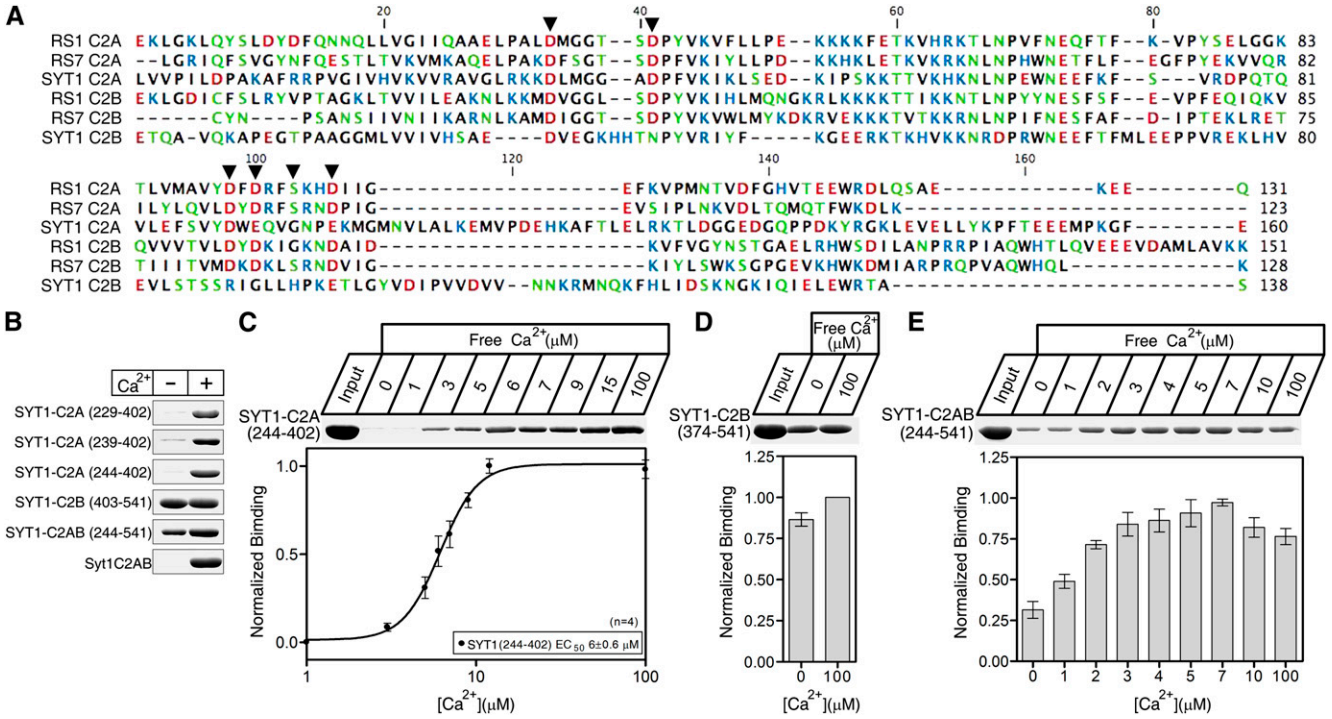

Figure 4. Ca^{2+}- and Phospholipid-Dependent Membrane Binding by SYT1.

(A) Sequence alignment of the C2 domains from rat synaptotagmin 1 (RS1), rat synaptotagmin 7 (RS7), and SYT1. Similar colors indicate similar polarity of the residues. Amino acid residues that form the Ca^{2+} binding sites of the C2 domains in rat synaptotagmin 1 and 7 are indicated by arrowheads.
(B) Recombinant GST fusion proteins containing the residues indicated were used in phospholipid binding assays. Proteins were incubated in the absence (−) or the presence (+) of 100 μM Ca^{2+} with liposomes composed of 25% PS/75% PC. Liposomes were precipitated by centrifugation, and bound proteins were analyzed by SDS-PAGE.
(C) to **(E)** The C2A domain **(C)**, C2B domain **(D)**, and C2AB domains **(E)** of SYT1 were incubated with liposomes as in **(B)** in the presence of the indicated concentrations of free Ca^{2+} (clamped with Ca^{2+}/EGTA buffers) to determine the half-maximal binding for free Ca^{2+}. The EC_{50} for SYT1-C2A was 6 ± 0.6 μM (paired *t* test, $P < 0.05$; $n = 4$). No binding was obtained when the liposomes were incubated in the presence of GST alone.

in the loss of membrane integrity. We then determined electrolyte leakage to quantify the extent of plasma membrane damage caused by increasing NaCl concentrations at high and low Ca^{2+} concentrations (Figure 5C). When growing in medium without NaCl and high Ca^{2+}, a higher percentage of electrolytes was lost from *syt1-2* seedlings compared with the wild type, indicating a reduced integrity of the plasma membrane of *syt1-2* even in standard conditions. This reduced plasma membrane integrity is comparable to that recently reported for the *Arabidopsis lew1* mutant affected in dolichol synthesis and abiotic stress tolerance (Zhang et al., 2008). Upon NaCl treatments, more electrolytes were lost from *syt1-2* plants, with the highest difference at 150 mM NaCl (Figure 5C). The decrease of extracellular Ca^{2+} in the medium caused a general decrease in membrane integrity of both *syt1-2* and wild-type seedlings at all conditions analyzed (Figure 5C). A time-course analysis using 150 mM NaCl indicated that at 4 h there was an important difference in electrolyte leakage between *syt1-2* plants and the wild type (see Supplemental Figure 5A online). These differences between *syt1-2* and wild-type seedlings persisted at 12 and 24 h of NaCl stress and were attenuated after 48 h of treatment.

If SYT1 plays a role in plasma membrane integrity, we hypothesized that other conditions that result in plasma membrane stress, such as osmotic shock or freezing, would produce an increased sensitivity of *syt1-2* plants. We treated *syt1-2* and wild-type seedlings with polyethylene glycol (PEG) to mimic drought stress as described previously (Xiong et al., 2001). Under control, 10%, or 20% PEG treatment, there was a small difference in the percentage of electrolyte leakage between wild-type and *syt1-2* plants (Figure 5D). However, at 30% PEG, significantly more electrolytes were lost from *syt1-2* seedlings than from the wild type. We then investigated if the reduced plasma membrane integrity of *syt1-2* was dependent on the tissue analyzed. As shown in Figure 5E, both root and shoots showed higher electrolyte leakage in *syt1-2* than in the wild type after 30% PEG treatment consistent with the ubiquitous expression of the *SYT1* gene (Figures 1E and 1F). Plasma membrane integrity of *syt1-2* and wild-type seedlings after freezing was then analyzed. As shown in Supplemental Figure 5B online, *syt1-2* seedlings showed lower membrane integrity than the wild type at control and subfreezing temperatures; however, these differences became apparent after freezing. Overall, we demonstrate that *syt1-2*

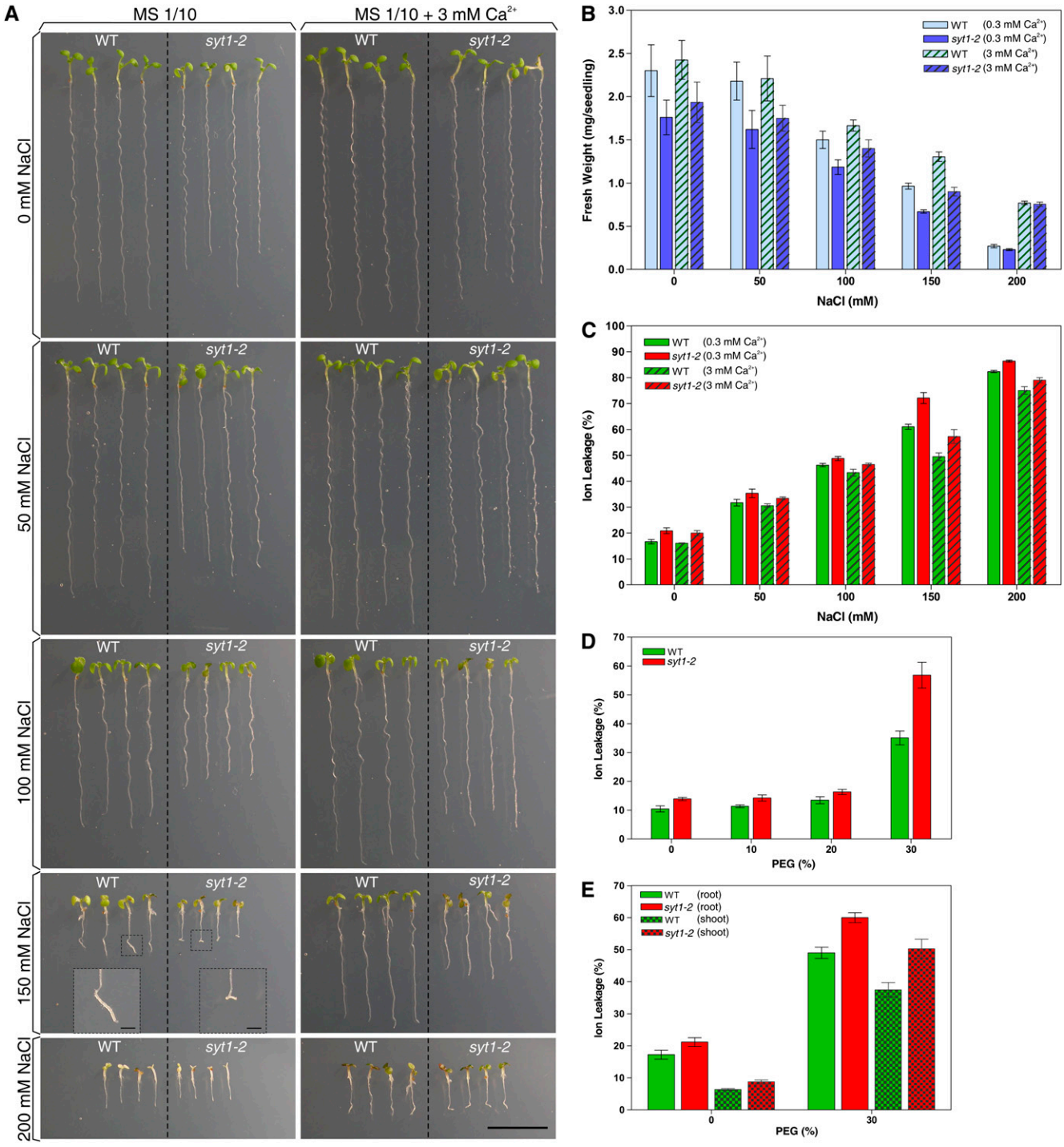

Figure 5. Physiological Characterization of the *syt1-2* Mutant.

(A) Phenotypes of wild-type and *syt1-2* seedlings growing at increasing NaCl concentrations. Wild-type and *syt1-2* seedlings were grown for 3 d in half-strength MS medium and then transferred to one-tenth MS medium at the Ca^{2+} and NaCl concentrations indicated and photographed 7 d later. The seedlings shown are representative of four independent trials. Bar = 10 mm; inset bars = 1 mm.

(B) Quantification of fresh weight for seedlings treated as described for **(A)**. For fresh weight determination, 12 seedlings were weighed at one time and the result was divided by 12. Data are means ± SE ($n = 4$). All mean values are significantly different between the wild type and *syt1-2* ($P < 0.05$) with the exception of the 200 mM NaCl treatment in which no significant differences were found.

(C) One-week-old seedlings grown in half-strength MS medium without NaCl were transferred to one-tenth MS medium plus the indicated NaCl and Ca^{2+}

seedlings present reduced plasma membrane integrity with respect to the wild type in control conditions that are enhanced under stress.

SYT1 Is Required for Maintenance of Plasma Membrane Integrity

Electrolyte leakage experiments indicate that both roots and shoots of *syt1-2* have reduced plasma membrane integrity (Figure 5E). Therefore, we studied plasma membrane integrity in vivo at cellular level using *Arabidopsis* roots, as this organ allows easy monitoring of cell membranes using confocal microscopy. We used the fluorescent dye FM4-64, a well-established endocytic marker (Samaj et al., 2005). It inserts into the lipid bilayer and labels the plasma membrane. Subsequently, it is taken up into the cell interior via endocytosis and gradually labels the entire endosomal network (Samaj et al., 2005; Dhonukshe et al., 2006). Fluorescence of a cell with a wounded plasma membrane after stress will increase many-fold owing to an unrestricted influx of the dye and a massive staining of the endomembrane network. This was tested in root cells following physical damage of *Arabidopsis* seedlings (Figure 6A) and further confirmed by the use of double labeling with fluorescein diacetate (FDA) and FM4-64 that distinguishes live from dead cells (Figure 6B).

For these experiments we used 3-d-old seedlings with a single root for reproducibility. We first investigated the effect of increasing concentrations of NaCl in membrane integrity after 1 h in wild-type and *syt1-2* roots. Because we have shown that low Ca^{2+} enhances the plasma membrane damage, we performed these experiments using low (0.3 mM) Ca^{2+} concentration. At control conditions (without NaCl) and up to 100 mM NaCl, no membrane damage was found in either wild-type or *syt1-2* roots (Figure 6C). At 120 mM NaCl, a few cells in *syt1-2* were completely stained with FM4-64, indicating disruption of their plasma membrane. The number of cells with damaged plasma membrane in *syt1-2* increased at higher concentrations of NaCl (Figure 6C). At 200 mM NaCl, while most cells were alive in wild-type roots, in *syt1-2*, only those cells located at the root tip were viable, indicating that the sensitivity of the plasma membrane was dependent on the cell type (Figure 6C). The use of double labeling with FDA and FM4-64 in these conditions further allowed us to clearly distinguish live from dead cells (Figure 6D).

We next analyzed plasma membrane integrity during a time-course experiment using 200 mM NaCl. We used this high NaCl concentration because it allows a continuous monitoring of plasma membrane damage of wild-type cells within a workable period of time. In control conditions, all cells from wild-type and *syt1-2* roots showed intact plasma membranes. After 30 min, all cells from the elongation region of *syt1-2* showed damaged plasma membrane, while only a few cells of wild-type roots were fully stained (see Supplemental Figure 6A online). In fact, as early as 30 s after the onset of the NaCl stress, we could observe lack of integrity of epidermal cells in *syt1-2* plants, indicating that this process occurs very rapidly and locally at the site of stress imposition (see Supplemental Figures 6B and 6C online). After 150 min, in contrast with the wild type, all cells in *syt1-2*, including meristematic cells, showed full staining indicative of total loss of viability.

To analyze at the cellular level the phenotype observed in conditions in which *syt1-2* and the wild type presented the main physiological differences (Figure 5A), we studied plasma membrane integrity of seedlings after 7 d of 150 mM NaCl treatment (Figure 6E). Whereas the main roots of *syt1-2* show very limited growth at 150 mM NaCl and low Ca^{2+}, wild-type roots were able to resume their growth (indicated by arrows in Figure 6E; see also Figure 5A, insets). FM4-64 staining showed that all cells in *syt1-2* roots were damaged, explaining their growth arrest (Figure 6E). Interestingly, most cells originated in wild-type roots after being transferred to NaCl (distinguishable by the thickening of the root) showed intact plasma membranes in contrast with those cells originated prior to the transfer to NaCl (Figure 6E). The most likely explanation is that meristematic cells of wild-type roots survive the NaCl shock and the newly formed cells are able to increase their membrane stability by adapting to the high NaCl conditions, thereby allowing root growth.

As we did previously for ion leakage measurements, we analyzed other osmotic agents to further demonstrate that the plasma membrane sensitivity of *syt1-2* is caused by the osmotic component of NaCl. Under control, 10% PEG, and 20% PEG treatment, no differences were found in wild-type and *syt1-2* roots (see Supplemental Figure 7A online). However, at 30% PEG, while most cells of wild-type roots showed intact plasma membranes, cells from the elongation region of *syt1-2* showed damaged plasma membranes. Similar results to those obtained using NaCl were observed when KCl was used as an osmotic agent (see Supplemental Figure 7B online).

We next investigated whether the loss of plasma membrane viability is a general outcome of mutants that are affected in abiotic stress tolerance. For this purpose, we used the previously identified *sos1* and *osm1/syp61 Arabidopsis* mutants. *sos1* shows hypersensitivity to NaCl, and the affected gene encodes a plasma membrane Na^+/H^+ antiporter (Shi et al., 2000). *osm1/syp6* shows reduced osmotic stress tolerance as a consequence of a mutation in a syntaxin gene (Zhu et al., 2002). As shown in Supplemental Figure 8 online, roots of *osm1/syp61* and *sos1*

Figure 5. (continued).

concentrations, and after 12 h electrolyte leakage was determined. Data are means of three independent assays. All mean values are significantly different between the wild type and *syt1-2* ($P < 0.05$).

(D) Ion leakage from 1-week-old seedlings treated with PEG. Data are means of three independent assays. All mean values are significantly different between the wild type and *syt1-2* ($P < 0.05$).

(E) Ion leakage from 1-week-old seedlings treated with PEG performed as in **(D)**, but root and shoot tissues were separated after PEG treatment. Data are means of three independent assays. All mean values are significantly different between the wild type and *syt1-2* ($P < 0.05$).

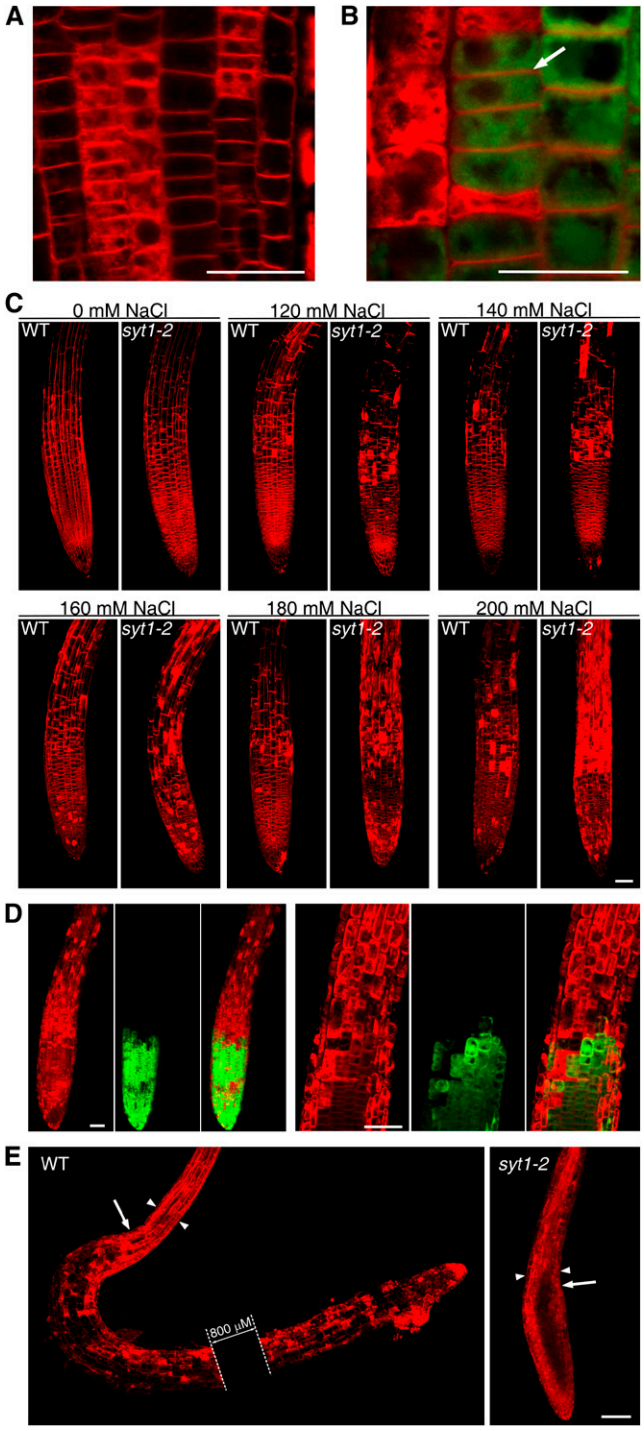

Figure 6. *syt1-2* Shows Reduced Cell Survival and Plasma Membrane Viability after NaCl Treatment.

(A) Massive staining of *Arabidopsis* root cells is the result of loss of plasma membrane integrity. A root from a wild-type plant was pressed between glass slides to induce mechanical damage and then stained with FM4-64. Bar = 25 μm.

(B) Double staining using FM4-64 and FDA. Viable cells that are stained in green by FDA show intact plasma membrane (arrow). Bar = 25 μm.

(C) Plasma membrane integrity analysis of *syt1-2* and wild-type roots by FM4-64 staining after 1 h of NaCl treatment. Representative roots from five independent experiments are shown. Bar = 50 μm.

(D) Roots of *syt1-2* after 1 h in 200 mM NaCl. The red (FM4-64) channel (left), the green (FDA) channel (middle), and the merged image (right) are shown. A closer view is shown in the right panel. Bars = 50 μm.

(E) Three-day-old seedlings grown in half-strength MS were transferred to one-tenth MS plates plus 150 mM NaCl. After 1 week of treatment, seedlings were stained with FM4-64. White arrows indicate the position of the root apex at the beginning of NaCl treatment. For illustration purposes, two images were joined (indicated by arrowheads) using Adobe Photoshop. Bar = 100 μm.

show similar plasma membrane sensitivity to their respective wild type after being exposed to NaCl stress. Taken together, these data indicate that reduced plasma membrane viability is not a general feature of abiotic stress hypersensitivity mutants.

DISCUSSION

In this study, we have identified the *syt1-2* mutant by its hypersensitivity to high NaCl. The reduced fitness of *syt1-2* seedlings was observed under control growing conditions but was highly enhanced with respect to the wild type under high osmolarity. These growth defects were evaluated at the cellular level by confocal microscopy, leading to the observation that the *syt1-2* mutant presented reduced plasma membrane integrity, which in turn causes a decrease in cell viability.

Based on current knowledge from the animal literature, there are two situations in which a defect in a single protein can result in an abnormally sensitive plasma membrane. It could be more susceptible to injury due to structural weakness, as occurs by defective components of the dystrophin-glycoprotein complex that are directly or indirectly involved in linking the cytoskeleton to the surrounding basement membrane (Ervasti et al., 1990; Duclos et al., 1998). Alternatively, the cell could have a defective plasma membrane repair mechanism as occurs by mutations in the C2-containing proteins syt7 (Reddy et al., 2001) and dysferlin (Bansal et al., 2003). In view of these two scenarios, the data we report here are in favor of a defective plasma membrane repair mechanism in the *syt1-2* mutant. A role in plasma membrane repair for SYT1 is also consistent with the results described in the accompanying article by Yamazaki et al. (2008), showing that *SYT1* is required for calcium-dependent freezing tolerance.

SYT1 protein shows structural and sequence homology to syt7, one of the components of the plasma membrane repair system in animals. We have demonstrated that *SYT1*, like *syt7*, shows ubiquitous expression. This is consistent with a possible role of SYT1 in a membrane repair process, since it is expected that plasma membrane repair must be maintained in most cells (Fukuda et al., 2002). Our biochemical studies confirm that SYT1 possesses functional C2 domains, a feature required for Ca^{2+}-dependent vesicular fusion (Fernández-Chacón et al., 2001). At the cellular level, we observed a higher degree of plasma membrane disruption in the *syt1-2* mutant compared with wild-type seedlings. We thus propose that SYT1 is a component of the

plasma membrane repair machinery in *Arabidopsis*, and the loss of SYT1 causes a reduction in membrane integrity, resulting in a general decrease in plant fitness that is enhanced under nonoptimal growing conditions. Most likely, the integrity of *syt1-2* plasma membranes is already affected under control conditions, reaching a level of damage earlier than the wild type under stress. A seemingly contradictory result is the finding that under control growing conditions, we did not observe damaged cells in roots using confocal microscopy. However, *syt1-2* always showed less growth rate than the wild type in these conditions, which was reflected by fresh weight quantification. We also demonstrated that a plasma membrane injury effectively occurs in control conditions by means of ion leakage measurements.

Localization of synaptotagmins has been critical to assign a function to these proteins. Roles for being Ca^{2+} sensors for neurotransmitter release and plasma membrane repair were originally proposed for syt1 and syt7 based on their localization in synaptic vesicles and lysosomes, respectively (Brose et al., 1992; Reddy et al., 2001). Therefore, SYT1 localization was analyzed by a variety of methods. We demonstrated its preferential plasma membrane localization and immunogold electron microscopy showed that young emerging cell walls of late cytokinetic cells have more abundant decoration of the plasma membrane with SYT1. These results are relevant for the proposed function of SYT1 because the cell plate suffers from internal mechanical stress as (after its fusion with the parent cell wall) it experiences the high turgor pressure while its mechanical stiffness is still weak (Baluska et al., 2006).

The Ca^{2+} binding affinity determined in vitro for the animal syt1 closely resembles physiological relevant concentrations in the presence of phospholipids (Geppert et al., 1994). Therefore, elucidating its Ca^{2+} binding mode and the mechanisms of its Ca^{2+}-dependent interactions has been essential for a better understanding of how syt1 regulates neurotransmitter release (Ubach et al., 1998). Here, we show that while the C2A domain of SYT1 is a canonical C2 domain in terms of phospholipid binding, the C2B domain exhibits a phospholipid binding in vitro that is independent of the presence of Ca^{2+}. It is conceivable that the constitutive lipid binding activity of SYT1 causes the docking of vesicles involved in repair via the C2B domain, thus facilitating the process. Alternatively, the C2B domain of SYT1 may bind constitutively to the plasma membrane (e.g., the *cis* membrane to which the protein is anchored via its transmembrane domain). Animal synaptotagmins also function in endocytosis, for example, in coupling exocytosis with the recycling of synaptic vesicles, as is the case for syt1 (Poskanzer et al., 2003). Furthermore, it has been recently shown that endocytosis promotes wound resealing by removing lesions from the plasma membrane (Idone et al., 2008). Therefore, a possibility to test in the future is that SYT1 could be involved in endocytosis of damaged membranes.

Interestingly, plasma membrane sensitivity to osmotic stress was dependent on cell type, as meristematic cells showed increased tolerance compared with cells located in the elongation zone. In sea urchin eggs, the resealing capacity is strongly dependent upon local availability of fusion-competent cytoplasmic organelles (McNeil and Steinhardt, 2003). Therefore, is possible that cells located within ~300 μm of the root apex, which are metabolically active and therefore engage in active vesicular trafficking, have a higher resealing capability. We believe that the observed difference in plasma membrane integrity under stress conditions is particularly important since the survival of meristematic cells allows the adaptation of daughter cells to stress.

Until recently, it was widely believed that biological membranes are naturally self-sealing, being able to repair lipid bilayer discontinuities without assistance. It is now clear that disruptions in the plasma membrane are repaired by an active, calcium-dependent process involving the exocytotic addition of internal membranes to the cell surface (McNeil and Kirchhausen, 2005; Bement et al., 2007). To our knowledge, there is little or no information on the molecular components involved in plasma membrane repair in plants. In fact, the occurrence of the process itself remains highly speculative, as several arguments support the idea that plasma membrane repair might not be necessary in plants. First, plant cells possess a rigid cell wall protecting the plasma membrane. Second, plant cells are not as mechanically active as muscle cells and therefore not prompted to physical injury. Third, the inherent plasticity of plants may allow the loss of important cells without endangering the entire organism. However, plants have to cope with numerous environmental challenges, such as wounding, freezing, drought, and salt stress, that can cause damage to the plasma membrane.

The molecular machinery regulating plasma membrane integrity in plants is essential for cell survival and likely involves a large number of components. The characterization of SYT1, the first plant member of such repair machinery, will facilitate the identification of other components and provide further understanding of the plasma membrane repair process.

METHODS

T-DNA Insertion Lines

The *Arabidopsis thaliana* ecotype $C24_{RD29a\text{-}LUC}$ T-DNA insertion lines (Ishitani et al., 1997) from which the *syt1-1* mutant was isolated were provided by J.K. Zhu (University of California, Riverside, CA). The *Arabidopsis* Col-0 T-DNA insertion mutant *syt1-2* (SAIL_775_A08) was identified using the SIGnAL website (http://signal.salk.edu) and was obtained from the ABRC.

Isolation of Salt-Hypersensitive Mutants

Preparation of the T-DNA–tagged *Arabidopsis* ecotype $C24RD_{29a\text{-}LUC}$ population and root-bending assay identification of salt-sensitive mutants were described previously (Zhu, 2002; Koiwa et al., 2006). Briefly, *Arabidopsis* seeds were sown onto MS agar medium, stratified for 3 d at 4°C, and then incubated at 23°C for 1 week. Seedlings were then transferred to basal medium supplemented with 160 mM NaCl, and root growth was scored 10 d later. DNA flanking the left border of the inserted T-DNA in *syt1-2* plants was isolated by thermal asymmetric interlaced PCR (Liu and Whittier, 1995) and subcloned into cloning vector pGEM-T Easy Vector system (Promega) according to the manufacturer's instructions. The entire isolated fragment was sequenced. The primers used in the thermal asymmetric interlaced PCR were specific for the T-DNA left border (*LB1*, 5′-ATACGACGGATCGTAATTTGTC-3′; *LB2*, 5′-TAATAACGCTGCGGACATCTAC-3′; and *LB3*, 5′-TTGACCATCATACTCATTGCTG-3′) and degenerate primers (*DEG1*, 5′-WGCNAGTNAGWANAA-3′; and *DEG2*, 5′-AWGCANGNCWGANATA-3′).

To isolate *syt1-2* plants homozygous for the T-DNA insertion, we used the following primer pairs: primer *SYT1DPCRR* (5′-TGGAAGCAA-GAAATTCGGTT-3′) was paired with the T-DNA–specific primer *SAIL LB3* (5′-TTCATAACCAATCTCGATACAC-3′) or with the primer *SYT1DPCRF* (5′-GTATAGGGGGAAGCTGGAGG-3′). Our molecular analyses indicated that the orientation of the T-DNA was in the opposite direction as indicated on the T-DNA Express website (http://signal.salk.edu/cgi-bin/tdnaexpress).

Salt Sensitivity

Seeds of the mutants and wild-type Col-0 were sown on half-strength MS medium, 1.5% (w/v) sucrose, and 1% (w/v) agar, stratified for 3 d at 4°C, and then incubated at 23°C under a 16-h-light/8-h-dark cycle for another 3 d. Seedlings were then transferred to one-tenth MS medium with NaCl added as described and to the same plates plus 3 mM $CaCl_2$.

Electrolyte Leakage Measurements

One-week-old seedlings grown in half-strength MS plates were transferred to one-tenth MS agar plates supplemented with the designated NaCl concentrations and to the same plates plus 3 mM $CaCl_2$. There were three replicates for each treatment. After the indicated times, seedlings were carefully removed from plates, washed with deionized water, and placed in tubes containing 5 mL of deionized water. The tubes were shaken overnight, and the conductivity of the solution was measured. The tubes with the seedlings were then autoclaved. After cooling down to room temperature, conductivities of the solutions were measured again. The percentage of electrolyte leakage was calculated as the percentage of the conductivity before autoclaving over that after autoclaving. Electrolyte leakage induced by PEG treatment was determined using 1-week-old seedlings grown in half MS agar plates as described previously (Xiong et al., 2001). Three independent experiments were done. For ion leakage measurements of roots and shoots after PEG treatment, we followed the same protocol as for whole seedlings, but shoots were excised from roots using a razor blade and treated separately. Ion leakage measurements after freezing were performed essentially as described (Nagao et al., 2008) with some modifications. One-week-old seedlings grown in half-strength MS plates were placed in the bottom of a test tube with 5 mL of deionized water. The portion of the test tubes that contained the samples was immersed in refrigerant (50% ethylene glycol) in a programmable cooling bath. The seedlings in the test tubes were equilibrated at 0°C for 10 min and frozen by seeding with ice. The samples were then equilibrated again at 0°C for 1 h and cooled at a rate of 1°C h^{-1} to the indicated temperatures. The test tubes were transferred to a refrigerator at 4°C in the dark after reaching the desired freezing temperature and allowed to thaw overnight. Nonfrozen control treatments (25 and 4°C) were maintained at the corresponding temperatures during the whole time of freezing procedure and overnight. After the treatments, the tubes were shaken for 2 h in the dark at room temperature and the conductivity of the solutions was measured. There were three replicates for each treatment.

RT-PCR Analyses

Total RNA was isolated using Trizol reagent (Life Technologies) according to the manufacturer's instructions, either from 10-d-old seedlings or from mature plants. Genomic DNA was removed by adding 5 units of DNase I (Gibco BRL) and incubated for 30 min at 37°C and then for 10 min at 70°C to inactivate the enzyme. For the first-strand cDNA synthesis, total RNA (1 μg) was used as template and the retrotranscription was performed using the SuperScript III first-strand synthesis system (Invitrogen). For PCR reactions, 1 μL of the synthesized cDNA was used as template. PCR was started at 95°C for 3 min followed by 25 cycles of 94°C (30 s) and 60°C (30 s). The following primers were used for the PCR reactions: *SYT1RTFw* (5′-ATTTGGGTTGAAGGCAACAG-3′) and *SYT1RTRv* (5′-CGATTTG-GATCTTTCCGTTC-3′). For an internal control, the constitutive gene tubulin β-5 chain (At1g20010) was used with the following primers: *tubulinF* (5′-CCTGATAACTTCGTCTTTGG-3′) and *tubulinR* (5′-GTG-AACTCCATCTCGTCCAT-3′).

Protein Gel Blot Analysis

Microsomal fractions were isolated from 3-week old Col-0 and *SYT1* plants grown in half-strength MS agar plates as described elsewhere (Schumaker and Sze, 1985). The protein concentration was determined with the BCA protein assay reagent (Pierce). Fifteen micrograms per sample were electrophoretically resolved in 12% Tris-HCl SDS gel (Bio-Rad) and transferred to the Protran transfer membrane (Schleicher and Schuell BioScience). The membranes were incubated for 1.5 h with an antiserum raised against synthetic peptides corresponding to C2A (amino acids 365 to 378) and C2B (amino acids 457 to 470) domains of SYT1. After 1.5 h of incubation with a secondary antibody conjugated with horseradish peroxidase (Sigma-Aldrich), the membranes were developed by ECL (GE Healthcare). Antibodies were produced against the SYT1 peptides RKTLDGGEDGQPPD and KKNRDPRWNEEFTF by GenScript (www.genscript.com).

Promoter GUS Analysis

For constructing the promoter:GUS fusion construct, genomic DNA from *Arabidopsis* ecotype Col-0 was extracted with a genomic DNA preparation kit (Qiagen), according to the manufacturer's instructions. A fragment of 1506 bp upstream from the translation start codon in the gene At2g20990 was amplified using the primers *SYT1For* (5′-GGGGACAAGTTTGTACAAAAAAGCAGGCTCATTGCTAGAGTGAA-AAGGGTTTAG-3′) and *SYT1Rev* (5′-GGGGACCACTTTGTACAAGA-AAGCTGGGTCTTTGATTTCCGTTTCAGATCCAAC-3′), which include the B1 and B2 recombination site sequences (Gateway). The SYT1 promoter was cloned using the Gateway system (Invitrogen) by first cloning into pDONR207, followed by cloning into the binary vector pBI101-G (a gift from P. Hussey, Durham University). The final vector was introduced into *Arabidopsis* by *Agrobacterium tumefaciens*–mediated transformation. GUS assays using transgenic T2 lines at different developmental stages were performed as described by Jefferson et al. (1987).

syt1-2 Complementation

For *syt1-2* complementation, the complete gene *At2g20990* was amplified using the following primers: *SYT1COMPF* (5′-AGGAATTCAA-GATCCTCTTGGT-3′) and *SYT1COMPR* (5′-TCGTCGACCATATATGA-TAGATAC-3′). The amplified genomic fragment was cloned into the binary vector pCAMBIA1300, and the recombinant plasmid was used to transform *A. tumefaciens* strain GV3101. The resulting *A. tumefaciens* transformants were used to transform *syt1-2* mutant plants. The resultant T1 plants were selected in half-strength MS medium supplemented with 50 mg/L hygromycin. The resistant plants were transferred and grown in soil. The homozygous identity of T-DNA insertion of the rescued plants was confirmed by PCR assay.

GFP constructs

To create the SYT1:GFP construct, the coding sequence of *SYT1* was PCR amplified using the primers *SYT1GFPFor* (5′-CACCATGGGCTTTT-TCAGTACGATACT-3′) and *SYT1GFPRev* (5′- TGCCATGGAAGAGG-CAGTTCGCCACTCG-3′) and cloned into the 35S-GFP-Nos carrying

expression vector pCAT-GFP (Reichel et al., 1996). For *A. tumefaciens*–mediated transformation, the complete expression cassette, 35S-SYT1:GFP:Nos, was excised and cloned into the binary vector pCB302 (Xiang et al., 1999).

The truncated SYT1 protein missing the N-terminal part (first 111 bp, 37 amino acids) of the protein was PCR amplified using the primers *deltaN-SYT1for* (5′-GCGGATCCTGAAATTCG-3′) and *deltaN-SYT1rev* (5′-GCACTAGTTCAAGAGGCAGTTCG-3′) and cloned into a modified pCAT-GFP vector, pCAT-GFPm3, in which the STOP codon was deleted. From the resulting vector, pCAT-GFPm3-ΔNSYT1, the expression cassette was subcloned into pCB302. The binary vectors where transformed into *A. tumefaciens* strain GV3101. *Arabidopsis* Col-0 was transformed, and selection for phosphinothricin resistance was performed on soil, spraying 2-week-old seedlings with 1 mL/L BASTA (Aventis). For ER labeling, tobacco (*Nicotiana tabacum*) leaves were transiently transformed with the vector pBINm-GFP5-ER (Haseloff et al., 1997).

Transformation of Tobacco Leaves

N. tabacum was grown on soil for 4 weeks at 25°C, and leaves were transiently transformed via *A. tumefaciens* leaf infiltration according to Batoko et al. (2000). The bacterial optical density (OD_{600}) used for infiltration was 0.05 for all constructs.

Microscopy

Seedlings of transgenic *Arabidopsis* were grown on vertically oriented half-strength MS Petri dishes. Three-day-old seedlings were mounted in liquid medium using a spacer of one layer of Parafilm between slide and cover slip or in similar slide growth chambers. For transiently transformed leaves of *N. tabacum*, pieces of ~1 cm^2 were cut out and mounted between slide and cover slip in tap water. For plasma membrane integrity analyses, *Arabidopsis* seeds were germinated in half-strength MS plates. Three-day-old seedlings were transferred to one-tenth MS supplemented with NaCl, KCl, or PEG 8000 at the described concentrations. After the corresponding treatment, seedlings were incubated with 50 μM FM4-64 for 3 min and mounted in one-tenth MS liquid medium using a spacer of one layer of cover slip between slide and cover slip for confocal microscopy.

The confocal microscopy was performed on a Leica SP5 confocal microscope, equipped with argon and krypton lasers. For excitation of GFP, the 488-nm line of the argon laser was used and emission was detected with the setting of the acousto optical beam splitter set to 500 to 560 nm. *Arabidopsis* and tobacco samples were examined using ×40 or ×16 oil immersion lenses. For detection of the green fluorescent dye FDA, the same settings as for GFP were used. The red fluorescent dye FM4-64 was excited by the 488-nm laser line, and emission was filtered between 620 and 710 nm. Projections of serial confocal sections and contrast enhancement were done using image processing software (Adobe Systems; Leica Application Suite Advanced Fluorescence; Leica Microsystems).

Generation and Purification of GST Fusion Proteins

RT-PCR of Col mRNA was used to produce GST fusion clones in pGEX-KG corresponding to the following SYT1 amino acid sequences: 229 to 402, 239 to 402, and 244 to 402, corresponding to the SYT1-C2A domain; 403 to 541, corresponding to the SYT1-C2B domain; and 244 to 541, corresponding to the SYT1-C2AB domain. Purification of GST fusion proteins was performed essentially as described (Guan and Dixon, 1991). Briefly, proteins expressed in BL21-RP were released by sonication and incubated with glutathione agarose beads (0.3 mL/L culture) overnight at 4°C. Proteins were washed on the agarose beads four times with 10 mL PBS, 1 mM EDTA, and 0.1 g/L PMSF. Purified protein was eluted from the agarose with 2.5 mL 100 mM Tris, pH 8.0, and 40 mM glutathione and concentrated to ~0.2 mL by centricon centrifugation (Millipore). Protein concentrations were determined by the method of Bradford (1976) with protein dye reagent concentrate from Bio-Rad, using BSA as standard.

Phospholipid Binding Assays

Phospholipid binding to isolated single C2 domains (C2A or C2B) and to the double C2 domain (C2AB) of SYT1 and syt1-C2AB was assessed by a centrifugation assay as described previously (Fernandez et al., 2001; Fernandez-Chacon et al., 2002; Shin et al., 2003). Briefly, phospholipids (PS/PC = 25/75, w/w) (Sigma-Aldrich) in chloroform were dried as a thin layer under a stream of nitrogen. Dried lipids were resuspended in buffer A (100 mM NaCl/50 mM HEPES, pH 6.8/4 mM EGTA) by vortexing for 20 min. Large multilamellar vesicles were collected by centrifugation for 20 min at 20,800*g* and resuspended in buffer A with various concentrations of free Ca^{2+} and used within 1 h. Calcium concentrations were calculated using the WEBMAXC program (http://www.stanford.edu/~cpatton/maxc.html). Purified soluble recombinant GST-C2 domains (6 μg) and vesicles (100 μg of phospholipids; total volume = 1 mL) were incubated for 15 min at 27°C with shaking at 250 rev/min on a platform shaker. Large multilamellar vesicles and bound protein were isolated by centrifugation for 10 min at 20,800*g* at 4°C. Pellets were washed three times with 0.5 mL of the corresponding incubation buffer, and the bound protein was analyzed by SDS-PAGE and densitometry using a Bio-Rad GS670 scanning densitometer of the Coomassie Brilliant Blue–stained gel.

Immunoflorescence Microscopy

Arabidopsis seedlings (Col-0) were grown on 1% phytagar plates, half-strength MS basal salts, 1.5% sucrose, pH 5.7, at 23°C and 16 h, 150 μE $m^{-2}s^{-1}$. Five-day-old seedlings were prepared for immunolocalization following the protocol by Vitha et al. (1997). Seedlings were fixed in 4% formaldehyde, embedded in PEG 400 distearate-1 hexadecanol, and sectioned. Sections were probed with either polyclonal anti-SYT1 antibody or preimmune serum, and antibody binding was subsequently visualized with Alexa Fluor 488–conjugated goat anti-rabbit antibody (Molecular Probes). After counterstaining by either 4',6-diamidino-2-phenylindole or propidium iodide, fluorescence images were examined with either Zeiss LSM 510 META or LEICA DMRB microscopes supplemented by a Hitachi HV-C20 camera controlled by a DISCUS microscopic program (Carl H. Hilgers, Technishes Büro). Images were processed using Adobe Photoshop CS.

Immunogold Electron Microscopy

Seedlings were fixed in 4% freshly prepared formaldehyde in MTSB buffer at 4°C for 6 h and then dehydrated through a graded ethanol series (also at 4°C) and embedded in LR White medium (Agar Scientific). Ultrathin sections were labeled by antibody against SYT1 and then with goat antirabbit IgG conjugated with 15-nm coloidal gold particles (Sigma-Aldrich). The sections were examined with a Zeiss LEO 912 AB transmission electron microscope.

Accession Numbers

Sequence data from this article can be found in the Arabidopsis Genome Initiative data library under accession number *At2g20990* (SYT1) and in the GenBank/EMBL data libraries under accession numbers NP_004191 (human syt7), EDM16756 (rat syt1), and AAA87725 (rat syt7). *syt1-2* is from the *Arabidopsis* SAIL collection (SAIL_775_A08).

Supplemental Data

The following materials are available in the online version of this article.

Supplemental Figure 1. Phenotypic Characterization of the *syt1-2* Mutant Allele and Genetic Complementation.

Supplemental Figure 2. Localization of the SYT1 Protein.

Supplemental Figure 3. Immunochemical Control Experiment Using Preimmune Serum.

Supplemental Figure 4. Ca^{2+}- and Phospholipid-Dependent Membrane Binding by Rat Synaptotagmin 1.

Supplemental Figure 5. Electrolyte Leakage of Wild-Type and *syt1-2* Seedlings upon NaCl and Freezing Treatments.

Supplemental Figure 6. Time-Course Analysis of Plasma Membrane Integrity upon NaCl Treatment.

Supplemental Figure 7. Polyethylene Glycol and KCl Produce Similar Effects as NaCl.

Supplemental Figure 8. *osm1* and *sos1* Mutants Show Similar Membrane Integrity as Wild-Type Plants.

ACKNOWLEDGMENTS

We thank our laboratory members for critical reading of the manuscript. We thank J. Rizo for his help in the phospholipid binding experiments and for critical reading of the manuscript. We thank J. Botella for critical reading of the manuscript. We thank T. Sudhof for the gift of the syt1-C2AB-GST construct. We also thank P.M. Hasegawa and R.A. Bressan for providing us with the *syt1-2* mutant and A. Esteban and D. Navas for technical assistance. A.L.S. was supported by a FPU fellowship from the Ministerio de Educación y Ciencia and F.B. by SAV Grant APVV-0432-06. This work was supported by funding from El Ministerio de Educación y Ciencia (Grants BIO2005-4733 and BIO2008-1709), grants from the Bundesministerium für Wirtschaft und Technologie via Deutsches Zentrum für Luft und Raumfahrt (Cologne, Germany; Project 50WB 0434), from the European Space Agency (ESA-ESTEC Noordwijk, The Netherlands; MAP Project AO-99-098), and from the Ente Cassa di Risparmio di Firenze (Italy).

Received October 16, 2008; revised November 6, 2008; accepted November 30, 2008; published December 16, 2008.

REFERENCES

Alexandersson, E., Saalbach, G., Larsson, C., and Kjellbom, P. (2004). Arabidopsis plasma membrane proteomics identifies components of transport, signal transduction and membrane trafficking. Plant Cell Physiol. **45:** 1543–1556.

Andrews, N. (2005). Membrane resealing: Synaptotagmin VII keeps running the show. Sci. STKE **2005:** pe19.

Andrews, N., and Chakrabarti, S. (2005). There's more to life than neurotransmission: The regulation of exocytosis by synaptotagmin VII. Trends Cell Biol. **15:** 626–631.

Baena-González, E., Rolland, F., Thevelein, J., and Sheen, J. (2007). A central integrator of transcription networks in plant stress and energy signalling. Nature **448:** 938–942.

Baluska, F., Menzel, D., and Barlow, P.W. (2006). Cytokinesis in plant and animal cells: Endosomes 'shut the door'. Dev. Biol. **294:** 1–10.

Baluska, F., Volkmann, D., and Menzel, D. (2005). Plant synapses: Actin-based domains for cell-to-cell communication. Trends Plant Sci. **10:** 106–111.

Bansal, D., Miyake, K., Vogel, S., Groh, S., Chen, C., Williamson, R., McNeil, P., and Campbell, K. (2003). Defective membrane repair in dysferlin-deficient muscular dystrophy. Nature **423:** 168–172.

Batoko, H., Zheng, H.Q., Hawes, C., and Moore, I. (2000). A rab1 GTPase is required for transport between the endoplasmic reticulum and Golgi apparatus and for normal golgi movement in plants. Plant Cell **12:** 2201–2218.

Bement, W., Yu, H., Burkel, B., Vaughan, E., and Clark, A. (2007). Rehabilitation and the single cell. Curr. Opin. Cell Biol. **19:** 95–100.

Bi, G., Alderton, J., and Steinhardt, R. (1995). Calcium-regulated exocytosis is required for cell membrane resealing. J. Cell Biol. **131:** 1747–1758.

Borsani, O., Cuartero, J., Valpuesta, V., and Botella, M.A. (2002). Tomato tos1 mutation identifies a gene essential for osmotic tolerance and abscisic acid sensitivity. Plant J. **32:** 905–914.

Borsani, O., Valpuesta, V., and Botella, M.A. (2003). Developing salt tolerant plants in a new century: a molecular biology approach. Plant Cell Tissue Organ Cult. **73:** 101–115.

Bradford, M.M. (1976). A rapid and sensitive method for the quantitation of microgram quantities of protein utilizing the principle of protein-dye binding. Anal. Biochem. **72:** 248–254.

Brose, N., Petrenko, A., Südhof, T., and Jahn, R. (1992). Synaptotagmin: A calcium sensor on the synaptic vesicle surface. Science **256:** 1021–1025.

Chinnusamy, V., Ohta, M., Kanrar, S., Lee, B., Hong, X., Agarwal, M., and Zhu, J. (2003). ICE1: A regulator of cold-induced transcriptome and freezing tolerance in Arabidopsis. Genes Dev. **17:** 1043–1054.

Coussens, L., Parker, P.J., Rhee, L., Yang-Feng, T.L., Chen, E., Waterfield, M.D., Francke, U., and Ullrich, A. (1986). Multiple, distinct forms of bovine and human protein kinase C suggest diversity in cellular signaling pathways. Science **233:** 859–866.

Craxton, M. (2004). Synaptotagmin gene content of the sequenced genomes. BMC Genomics **5:** 43.

Craxton, M. (2007). Evolutionary genomics of plant genes encoding N-terminal-TM-C2 domain proteins and the similar FAM62 genes and synaptotagmin genes of metazoans. BMC Genomics **8:** 259.

Dai, H., Shin, O., Machius, M., Tomchick, D., Südhof, T., and Rizo, J. (2004). Structural basis for the evolutionary inactivation of Ca^{2+} binding to synaptotagmin 4. Nat. Struct. Mol. Biol. **11:** 844–849.

Dhonukshe, P., Baluska, F., Schlicht, M., Hlavacka, A., Samaj, J., Friml, J., and Gadella, T. (2006). Endocytosis of cell surface material mediates cell plate formation during plant cytokinesis. Dev. Cell **10:** 137–150.

Duclos, F., et al. (1998). Progressive muscular dystrophy in alpha-sarcoglycan-deficient mice. J. Cell Biol. **142:** 1461–1471.

Ervasti, J., Ohlendieck, K., Kahl, S., Gaver, M., and Campbell, K. (1990). Deficiency of a glycoprotein component of the dystrophin complex in dystrophic muscle. Nature **345:** 315–319.

Fernandez, I., Arac, D., Ubach, J., Gerber, S.H., Shin, O., Gao, Y., Anderson, R.G., Sudhof, T.C., and Rizo, J. (2001). Three-dimensional structure of the synaptotagmin 1 C2B-domain: Synaptotagmin 1 as a phospholipid binding machine. Neuron **32:** 1057–1069.

Fernández-Chacón, R., Königstorfer, A., Gerber, S., García, J., Matos, M., Stevens, C., Brose, N., Rizo, J., Rosenmund, C., and Südhof, T. (2001). Synaptotagmin I functions as a calcium regulator of release probability. Nature **410:** 41–49.

Fernández-Chacón, R., Shin, O., Königstorfer, A., Matos, M., Meyer, A., Garcia, J., Gerber, S., Rizo, J., Südhof, T., and Rosenmund, C. (2002). Structure/function analysis of Ca^{2+} binding to the C2A domain of synaptotagmin 1. J. Neurosci. **22:** 8438–8446.

Fernandez-Chacon, R., Shin, O.H., Konigstorfer, A., Matos, M.F.,

Meyer, A.C., Garcia, J., Gerber, S.H., Rizo, J., Sudhof, T.C., and Rosenmund, C. (2002). Structure/function analysis of Ca^{2+} binding to the C2A domain of synaptotagmin 1. J. Neurosci. **22:** 8438–8446.

Fukuda, M., Ogata, Y., Saegusa, C., Kanno, E., and Mikoshiba, K. (2002). Alternative splicing isoforms of synaptotagmin VII in the mouse, rat and human. Biochem. J. **365:** 173–180.

Geppert, M., Goda, Y., Hammer, R., Li, C., Rosahl, T., Stevens, C., and Südhof, T. (1994). Synaptotagmin I: A major Ca^{2+} sensor for transmitter release at a central synapse. Cell **79:** 717–727.

Guan, K.L., and Dixon, J.E. (1991). Eukaryotic proteins expressed in *Escherichia coli*: An improved thrombin cleavage and purification procedure of fusion proteins with glutathione S-transferase. Anal. Biochem. **192:** 262–267.

Hasegawa, P.M., Bressan, R.A., Zhu, J.K., and Bohnert, H.J. (2000). Plant cellular and molecular responses to high salinity. Annu. Rev. Plant Physiol. Plant Mol. Biol. **51:** 463–499.

Haseloff, J., Siemering, K.R., Prasher, D.C., and Hodge, S. (1997). Removal of a cryptic intron and subcellular localization of green fluorescent protein are required to mark transgenic Arabidopsis plants brightly. Proc. Natl. Acad. Sci. USA **94:** 2122–2127.

Idone, V., Tam, C., Goss, J.W., Toomre, D., Pypaert, M., and Andrews, N.W. (2008). Repair of injured plasma membrane by rapid Ca^{2+}-dependent endocytosis. J. Cell Biol. **180:** 905–914.

Ishitani, M., Xiong, L., Stevenson, B., and Zhu, J.K. (1997). Genetic analysis of osmotic and cold stress signal transduction in Arabidopsis: Interactions and convergence of abscisic acid-dependent and abscisic acid-independent pathways. Plant Cell **9:** 1935–1949.

Jefferson, R.A., Kavanagh, T.A., and Bevan, M.W. (1987). GUS fusions: Beta-glucuronidase as a sensitive and versatile gene fusion marker in higher plants. EMBO J. **6:** 3901–3907.

Kawamura, Y., and Uemura, M. (2003). Mass spectrometric approach for identifying putative plasma membrane proteins of Arabidopsis leaves associated with cold acclimation. Plant J. **36:** 141–154.

Koiwa, H., Bressan, R.A., and Hasegawa, P.M. (2006). Identification of plant stress-responsive determinants in Arabidopsis by large-scale forward genetic screens. J. Exp. Bot. **57:** 1119–1128.

Liu, J., Ishitani, M., Halfter, U., Kim, C., and Zhu, J. (2000). The *Arabidopsis thaliana* SOS2 gene encodes a protein kinase that is required for salt tolerance. Proc. Natl. Acad. Sci. USA **97:** 3730–3734.

Liu, J., and Zhu, J.K. (1998). A calcium sensor homolog required for plant salt tolerance. Science **280:** 1943–1945.

Liu, Y.G., and Whittier, R.F. (1995). Thermal asymmetric interlaced PCR: Automatable amplification and sequencing of insert end fragments from P1 and YAC clones for chromosome walking. Genomics **25:** 674–681.

McNeil, P., and Kirchhausen, T. (2005). An emergency response team for membrane repair. Nat. Rev. Mol. Cell Biol. **6:** 499–505.

McNeil, P., and Steinhardt, R. (2003). Plasma membrane disruption: Repair, prevention, adaptation. Annu. Rev. Cell Dev. Biol. **19:** 697–731.

Mishra, G.R., et al. (2006). Human protein reference database – 2006 update. Nucleic Acids Res. **34:** D411–D414.

Miyake, K., and McNeil, P.L. (1995). Vesicle accumulation and exocytosis at sites of plasma membrane disruption. J. Cell Biol. **131:** 1737–1745.

Nagao, M., Arakawa, K., Takezawa, D., and Fujikawa, S. (2008). Long- and short-term freezing induce different types of injury in *Arabidopsis thaliana* leaf cells. Planta **227:** 477–489.

Poskanzer, K., Marek, K., Sweeney, S., and Davis, G. (2003). Synaptotagmin I is necessary for compensatory synaptic vesicle endocytosis in vivo. Nature **426:** 559–563.

Reddy, A., Caler, E., and Andrews, N. (2001). Plasma membrane repair is mediated by Ca^{2+}-regulated exocytosis of lysosomes. Cell **106:** 157–169.

Reichel, C., Mathur, J., Eckes, P., Langenkemper, K., Koncz, C., Schell, J., Reiss, B., and Maas, C. (1996). Enhanced green fluorescence by the expression of an *Aequorea victoria* green fluorescent protein mutant in mono- and dicotyledonous plant cells. Proc. Natl. Acad. Sci. USA **93:** 5888–5893.

Rosado, A., Amaya, I., Valpuesta, V., Cuartero, J., Botella, M., and Borsani, O. (2006a). ABA- and ethylene-mediated responses in osmotically stressed tomato are regulated by the TSS2 and TOS1 loci. J. Exp. Bot. **57:** 3327–3335.

Rosado, A., Schapire, A., Bressan, R., Harfouche, A., Hasegawa, P., Valpuesta, V., and Botella, M. (2006b). The Arabidopsis tetratricopeptide repeat-containing protein TTL1 is required for osmotic stress responses and abscisic acid sensitivity. Plant Physiol. **142:** 1113–1126.

Rubio, L., Rosado, A., Linares-Rueda, A., Borsani, O., Garcia-Sanchez, M.J., Valpuesta, V., Fernandez, J.A., and Botella, M.A. (2004). Regulation of K^+ transport in tomato roots by the TSS1 locus. Implications in salt tolerance. Plant Physiol. **134:** 452–459.

Sagi-Eisenberg, R. (2007). The mast cell: Where endocytosis and regulated exocytosis meet. Immunol. Rev. **217:** 292–303.

Samaj, J., Read, N.D., Volkmann, D., Menzel, D., and Baluska, F. (2005). The endocytic network in plants. Trends Cell Biol. **15:** 425–433.

Schumaker, K.S., and Sze, H. (1985). A Ca/H antiport system driven by the proton electrochemical gradient of a tonoplast H-ATPase from oat roots. Plant Physiol. **79:** 1111–1117.

Shao, X., Davletov, B., Sutton, R., Südhof, T., and Rizo, J. (1996). Bipartite Ca^{2+}-binding motif in C2 domains of synaptotagmin and protein kinase C. Science **273:** 248–251.

Shi, H., Ishitani, M., Kim, C., and Zhu, J.K. (2000). The *Arabidopsis thaliana* salt tolerance gene SOS1 encodes a putative Na^+/H^+ antiporter. Proc. Natl. Acad. Sci. USA **97:** 6896–6901.

Shin, O.H., Rhee, J.S., Tang, J., Sugita, S., Rosenmund, C., and Sudhof, T.C. (2003). Sr^{2+} binding to the Ca^{2+} binding site of the synaptotagmin 1 C2B domain triggers fast exocytosis without stimulating SNARE interactions. Neuron **37:** 99–108.

Steinhardt, R.A., Bi, G., and Alderton, J.M. (1994). Cell membrane resealing by a vesicular mechanism similar to neurotransmitter release. Science **263:** 390–393.

Sudhof, T. (2004). The synaptic vesicle cycle. Annu. Rev. Neurosci. **27:** 509–547.

Südhof, T. (2001). Synaptotagmins: Why so many? J. Biol. Chem. **277:** 7629–7632.

Sutton, R., Davletov, B., Berghuis, A., Südhof, T., and Sprang, S. (1995). Structure of the first C2 domain of synaptotagmin I: A novel Ca^{2+}/phospholipid-binding fold. Cell **80:** 929–938.

Tang, J., Maximov, A., Shin, O., Dai, H., Rizo, J., and Südhof, T. (2006). A complexin/synaptotagmin 1 switch controls fast synaptic vesicle exocytosis. Cell **126:** 1175–1187.

Ubach, J., Zhang, X., Shao, X., Südhof, T., and Rizo, J. (1998). Ca^{2+} binding to synaptotagmin: How many Ca^{2+} ions bind to the tip of a C2-domain? EMBO J. **17:** 3921–3930.

Vitha, S., Baluska, F., Mews, M., and Volkmann, D. (1997). Immunofluorescence detection of F-actin on low melting point wax sections from plant tissues. J. Histochem. Cytochem. **45:** 89–95.

Xiang, C., Han, P., Lutziger, I., Wang, K., and Oliver, D.J. (1999). A mini binary vector series for plant transformation. Plant Mol. Biol. **40:** 711–717.

Xiong, L., Lee, B., Ishitani, M., Lee, H., Zhang, C., and Zhu, J.K. (2001). FIERY1 encoding an inositol polyphosphate 1-phosphatase is

a negative regulator of abscisic acid and stress signaling in Arabidopsis. Genes Dev. **15:** 1971–1984.

Xiong, L., and Zhu, J. (2001). Abiotic stress signal transduction in plants: Molecular and genetic perspectives. EMBO J. **112:** 152–166.

Yamazaki, T., Kawamura, Y., Minami, A., and Uemura, M. (2008). Calcium-dependent freezing tolerance in *Arabidopsis* involves membrane resealing via synaptotagmin SYT1. Plant Cell **20:** 3389–3404.

Zhang, H., Ohyama, K., Boudet, J., Chen, Z., Yang, J., Zhang, M., Muranaka, T., Maurel, C., Zhu, J.K., and Gong, Z. (2008). Dolichol biosynthesis and its effects on the unfolded protein response and abiotic stress resistance in Arabidopsis. Plant Cell **20:** 1879–1898.

Zhu, J., Fu, X., Koo, Y., Zhu, J., Jenney, F., Adams, M., Zhu, Y., Shi, H., Yun, D., Hasegawa, P., and Bressan, R. (2007). An enhancer mutant of Arabidopsis salt overly sensitive 3 mediates both ion homeostasis and the oxidative stress response. Mol. Cell. Biol. **27:** 5214–5224.

Zhu, J., Gong, Z., Zhang, C., Song, C.P., Damsz, B., Inan, G., Koiwa, H., Zhu, J.K., Hasegawa, P.M., and Bressan, R.A. (2002). OSM1/SYP61: A syntaxin protein in Arabidopsis controls abscisic acid-mediated and non-abscisic acid-mediated responses to abiotic stress. Plant Cell **14:** 3009–3028.

Zhu, J.K. (2002). Salt and drought stress signal transduction in plants. Annu. Rev. Plant Physiol. Plant Mol. Biol. **53:** 247–273.

Zimmermann, P., Hirsch-Hoffmann, M., Hennig, L., and Gruissem, W. (2004). GENEVESTIGATOR. Arabidopsis microarray database and analysis toolbox. Plant Physiol. **136:** 2621–2632.